

## Real surface area of the aluminium electrode in sodium chloride solution

D. M. DRAŽIĆ,<sup>1</sup> J. P. POPIĆ<sup>1</sup> and Z. RAKOČEVIĆ<sup>2</sup>

<sup>1</sup>*Institute of Electrochemistry ICTM, Njegoševa 12, P.O.Box 815, YU-11001 Belgrade, and*  
<sup>2</sup>*Vinča Institute of Nuclear Sciences, P.O.Box 522, YU-11001 Belgrade, Yugoslavia*

(Received 10 July 1999)

By combining the techniques of electrochemical slow potentiodynamic, AC impedance and atomic force microscopy (AFM), it was shown that the differences in the anodic dissolution rates of Al in 0.5 NaCl solutions as measured experimentally in the potential region between the corrosion and pitting potential, are mainly due to differences in surface roughness of the electrodes used. It was shown that mechanical grinding and polishing of the electrode surface with emery paper (400 grit) and alumina polishing powder ( $\varnothing$  0.25  $\mu\text{m}$ ) can produce surfaces differing by a factor of 6 in the roughness factor  $R_a$ . By using AFM estimates of the roughness factors a true electrode capacitance of 4.63  $\mu\text{C cm}^{-2}$  and thickness  $d_{\text{ox}} \approx 2.0$  nm for the barrier layer of the surface film was estimated. The outer part of the film is porous, partly as amorphous  $\text{Al}(\text{OH})_3$ , or crystalline bayerite ( $\text{Al}_2\text{O}_3 \cdot 3\text{H}_2\text{O}$ ).

*Key words:* aluminium, corrosion, real surface area, oxide thickness.

It has been shown by several authors<sup>1-4</sup> that anodic dissolution of high purity aluminium in deaerated neutral sodium chloride solutions follows Tafel like behavior in the potential range between the corrosion,  $E_{\text{cor}}$ , and pitting potential,  $E_{\text{pit}}$ , with rather high slope values. In previous papers,<sup>5,6</sup> we have also reported high Tafel slopes of *ca.* 400  $\text{mV dec}^{-1}$  in this potential region. These high Tafel slopes indicate that the anodic process of Al dissolution could be due to slow ionic transport through the oxide film.<sup>7</sup> However, we pointed out that the same behavior could be observed if charge transfer at either the metal/oxide or the oxide/solution interface controls the dissolution rate.<sup>5</sup>

A large amount of literature is devoted to the electrochemistry of thick oxide films formed by anodization of aluminium for protective purposes and also to the rather thick barrier oxide films formed in borate or similar electrolytes prepared for use in electric capacitors.

Spontaneously formed oxide films on Al in contact with humid air or electrolytes are rather thin and to some extent more complex in structure than the previously mentioned thick films. During contact of Al with water, and in particular neutral

sodium chloride solutions, some changes in the properties of the oxide layer occurs. Hart<sup>8</sup> and Alwitt<sup>9,10</sup> showed that in contact with water a sandwich type film forms, consisting of a compact barrier type  $\text{Al}_2\text{O}_3$  layer closer to the metal and a porous amorphous  $\text{Al}(\text{OH})_3$  on the solution side. With time this outer layer slowly transforms into crystalline boehmit ( $\text{Al}_2\text{O}_3 \cdot \text{H}_2\text{O}$ ) and later on to crystalline bayerit ( $\text{Al}_2\text{O}_3 \cdot 3\text{H}_2\text{O}$ ). Alwitt<sup>9</sup> also showed that this transformation occurs rapidly if the temperature is raised above 60 °C.

Our previous results<sup>5,11</sup> show that the change in the thickness and properties of the amorphous part of the oxide layer have practically no influence on the rate of anodic dissolution of Al in the potential region  $E_{\text{cor}} - E_{\text{pit}}$ . On the other hand, an increase in the thickness of the barrier layer decreases the anodic dissolution rate. However, the correlations between the thickness of the film and the registered current densities presented by different authors<sup>2,11</sup> might be questioned on the ground that the roughness factors were unknown, and might be different for differently prepared electrode surfaces. At the same time, the problem of the determination of the real surface area is very difficult.<sup>13</sup>

The purpose of this work was to attempt to determine the real surface area of Al electrodes in 0.5 M NaCl solution, the real electrode capacitances and the real thickness of the barrier part of the oxide film by combining electrochemical and atomic force microscopy (AFM) measurements.

## EXPERIMENTAL

Experiments were performed with high purity Al (Alcane, 99.999%) in deaerated 0.5 M aqueous NaCl solution in a glass electrochemical cell purged with purified nitrogen. A Pt wire was the counter electrode while a saturated calomel electrode (SCE) served as the reference electrode. Merck p.a. chemicals and doubly distilled water were used for the preparation of the solutions.

The experiments were performed at room temperature (22 °C). All the potentials are referred to SCE. The Al electrode surface (geometric working area 1 cm<sup>2</sup>) was prepared by mechanical polishing with polishing material of different grain size: SiC papers of 400 and 1000 grit and water suspensions of alumina powder of 1.0, 0.25 and 0.05  $\mu\text{m}$ . After polishing the surfaces were washed in water in an ultrasonic bath.

Anodic polarization curves were obtained by a very slow (1 mV s<sup>-1</sup>) potential sweep technique (PINE Instrument Company-RDE 4) while the electrode capacitances were determined by the AC impedance technique (PAR 273 potentiostat coupled with PAR 5301 lock-in amplifier and a PC computer). For microscope surface studies an atomic force microscope (Quesant Scops) was used. The surface roughness ( $R_a$ ) obtained from the AFM profiles, is defined as the square root of the mean square of the deviation of the peaks and troughs from the mean surface level and calculated by a corresponding AFM computing program.

## RESULTS

### *Electrode capacitance*

The images obtained using AFM showed considerable roughness (see Figs. 1–3) which decreased when finer polished agents were used. The measured electrode capacitances increased with increasing roughness factor of the electrodes used, as shown in Fig. 4. This function is linear allowing its extrapolation to zero roughness,

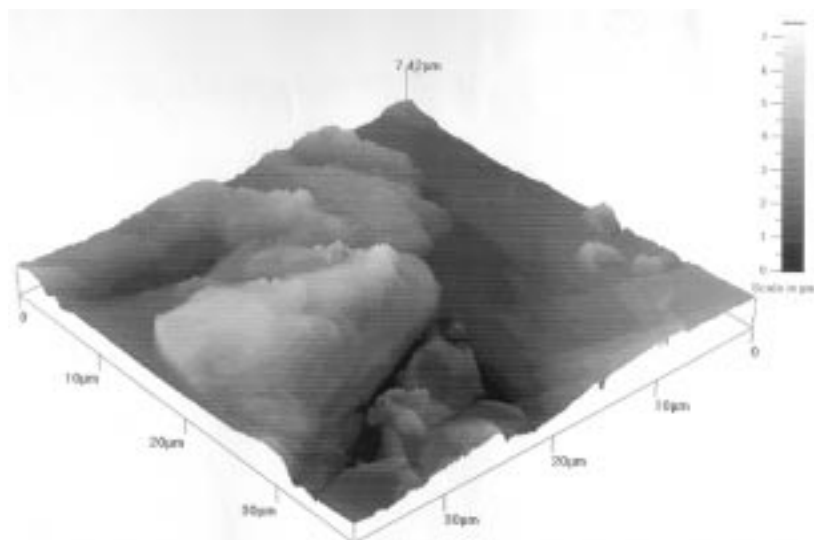


Fig. 1. AFM 3D image of an Al surface grinded with 400 grit emery paper.  $R_a = 687$  nm.

$R_a = 0$  (*i.e.*, an ideally flat surface). The extrapolated electrode capacitance (*i.e.*, total capacitance of the interphase metal/film/electrolyte) is  $C_T = 3.76 \mu\text{F cm}^{-2}$ .

The electrode capacitances were measured also, for electrodes mechanically prepared in the same way (polishing with  $\text{Al}_2\text{O}_3$ ,  $\varnothing 1 \mu\text{m}$ ) but afterwards treated differently, prior to capacitance measurement in a NaCl solution. Figure 5 depicts the capacitance data as a function of time for differently prepared electrodes: 1. –

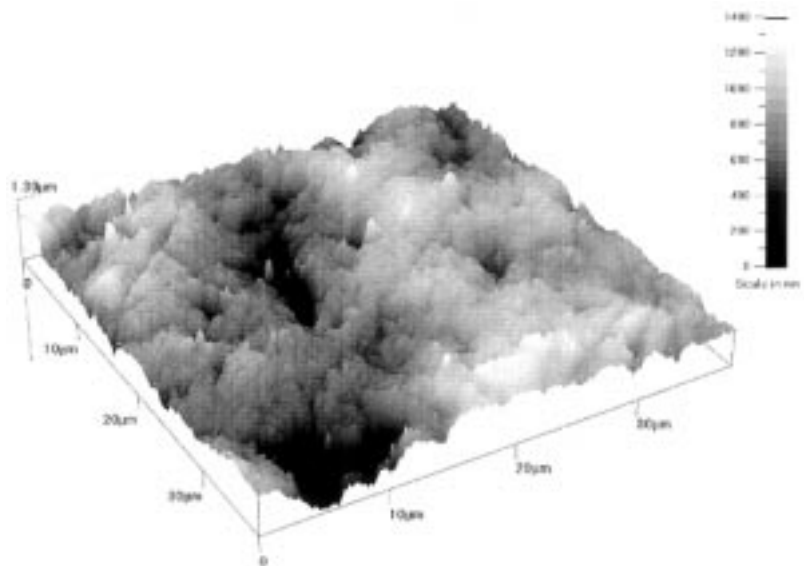


Fig. 2. AFM 3D image of an Al surface polished with a  $\varnothing 0.25 \mu\text{m}$   $\text{Al}_2\text{O}_3$  suspension.  $R_a = 185$  nm.

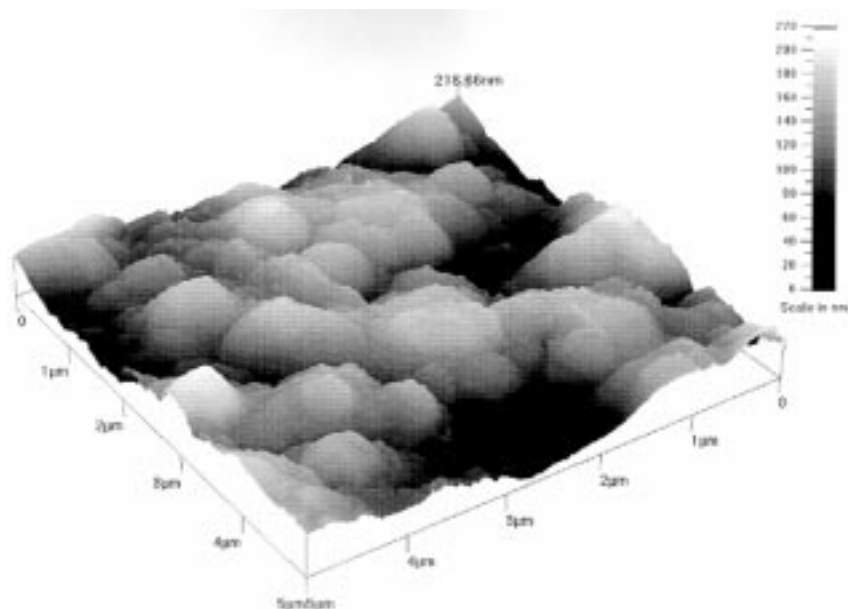


Fig. 3. AFM 3D image of an Al surface polished with a  $\varnothing$  0.05  $\mu\text{m}$   $\text{Al}_2\text{O}_3$  suspension.  $R_a = 120$  nm.

only mechanically polished (used here as a reference); 2.– after boiling the polished electrode for 10 min in distilled water to provoke crystallization of the amorphous surface layer to crystalline bayerite; 3.– after cathodic polarization with  $10 \text{ mA cm}^{-2}$  for 5 min, which caused the so called alkaline corrosion<sup>8</sup> of Al (due to the dissolution of the oxide film in the locally alkalized solution caused by  $\text{H}_2$  evolution), and 4.–

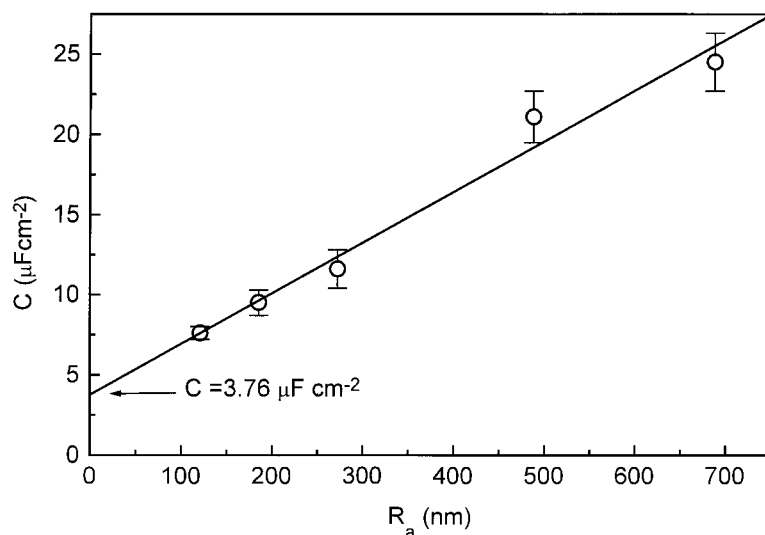


Fig. 4. Al electrode capacitance in deaerated 0.5 M NaCl solution as a function of electrode surface roughness ( $R_a$ ).

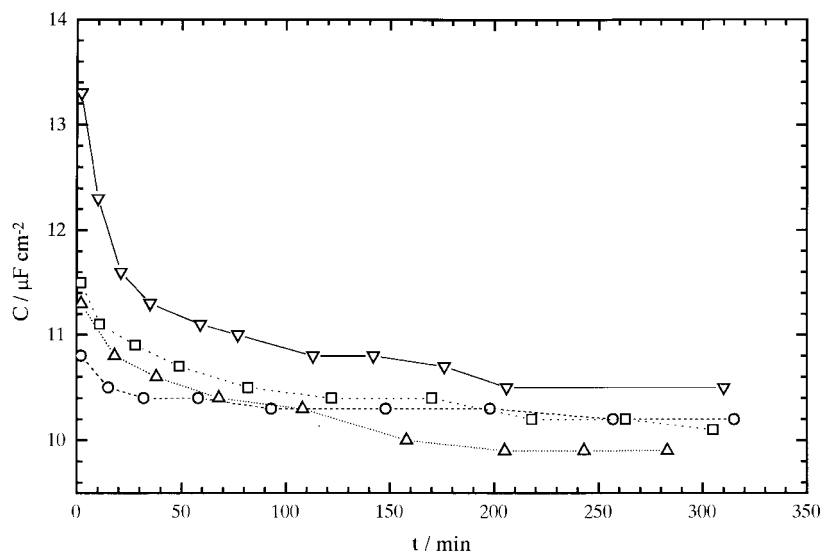


Fig. 5. Al electrode capacitance in 0.5 M NaCl solution as a function of time for electrodes polished with  $\text{Ø } 1 \mu\text{m Al}_2\text{O}_3$  but treated differently afterwards: (o) no further treatment; ( $\Delta$ ) after boiling in distilled water for 5 min, ( $\nabla$ ) after prolonged cathodic polarization, and ( $\square$ ) after contact with pure water for 192 h.

after the polished surface had been left for 192 h in distilled water prior to the measurements.

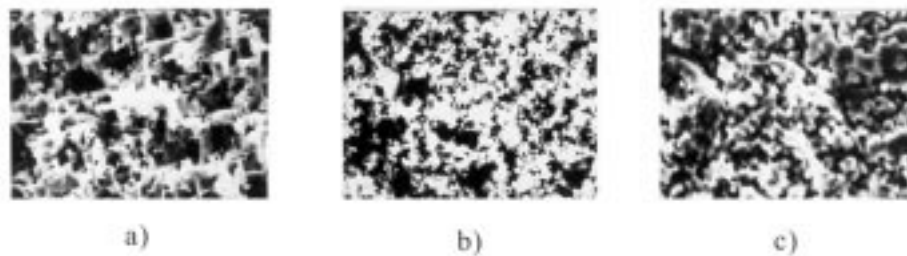


Fig. 6. Microphotographs of an Al surface after 30 min of anodic dissolution with  $300 \text{ mA cm}^{-2}$  in 0.5 M NaCl solution: a) immediately after the experiment, b) after such a surface had been in contact only with water for 24 h, and c) the same but after 88 h. Magnification: 600 x.

As can be seen, except for the cathodically pretreated surfaces, all others, in a rather short time after equilibration of the oxide layer with NaCl solution, attained practically the same capacitance value of *ca.*  $10 \mu\text{F cm}^{-2}$ . Only the cathodically pretreated surface initially showed somewhat higher capacitances (due to the removal of the oxide film), but after *ca.* 60 min similar capacitance values as the other electrodes were also attained. This simply indicates that the, by alkaline corrosion attacked oxide surface, healed itself and became practically identical to

all others. Similarly, keeping the electrodes in distilled water for a long time, which affects the structure of the amorphous (and porous) part of the film<sup>8,10</sup> does not affect the electrode capacitance, being  $C_{\text{ox}} = 11.9 \mu\text{F cm}^{-2}$ , obtained as the mean value of five independent experiments. On the other hand, the electrode capacitance of the surface which underwent anodic polarization at potentials more positive than  $E_{\text{pit}}$ , *i.e.*, at higher current densities, were much higher. For example, the electrode polarized with  $300 \text{ mA cm}^{-2}$  for 30 min had a capacitance of  $62 \mu\text{F cm}^{-2}$ . Of course, this is due to the large increase of the surface area caused by pitting, as depicted on the microphotographs in Fig. 6.

#### Anodic polarization

Anodic polarization curves for the electrodes having different surface roughnesses are shown in Fig. 7. It is clear that the electrodes with higher  $R_a$  values dissolve faster, *i.e.*, at constant potential the dissolution currents are higher. Obviously, this is the result of the increase in real surface area. For example, as shown in Fig. 8, the effective anodic current density at  $-0.9 \text{ V}$  is a linear function of  $R_a$ , which extrapolated to  $R_a = 0$  gives  $j_a = 0.55 \mu\text{A cm}^{-2}$ , as the true anodic current density of an ideally flat surface. The same can be done for any other electrode potential in the  $E_{\text{cor}} - E_{\text{pit}}$  range. For example, Fig. 9 shows again the linear dependence of  $j_a$  on  $R_a$ , which after extrapolation gives  $j_a = 0.8 \text{ mA cm}^{-2}$  as the dissolution rate at  $E_{\text{pit}}$  of an ideally flat surface just before pitting commences.

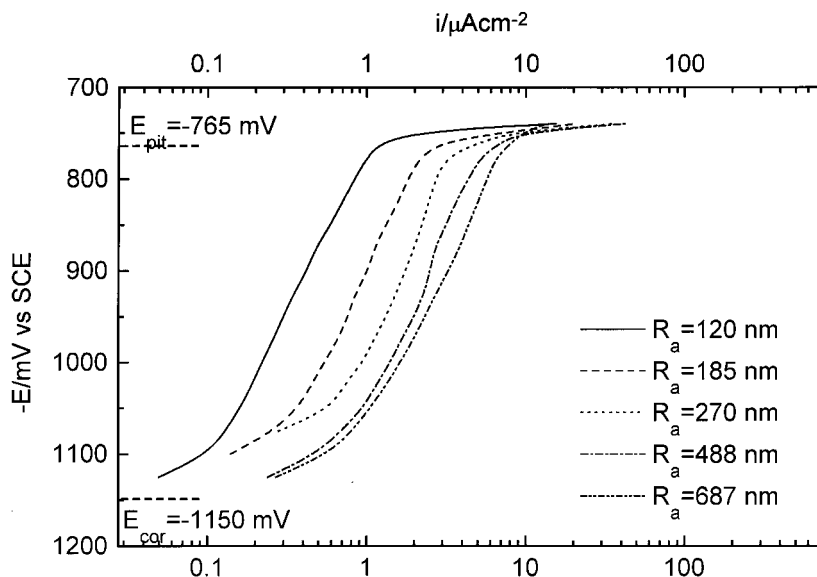


Fig. 7. Anodic polarization curves for Al electrodes of different surface roughnesses in deaerated  $0.5 \text{ M NaCl}$  solution. Sweep rate  $1 \text{ mV s}^{-1}$ .

The microphotographs in Fig. 6 also show that prolonged exposure of Al to distilled water results in a thickening of the amorphous layer, but this does not affect

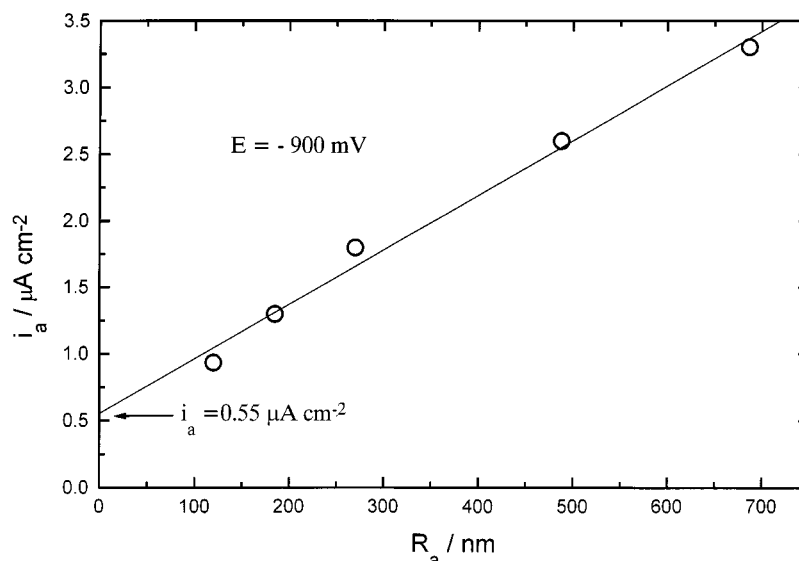


Fig. 8. Anodic dissolution current of Al electrodes in deaerated 0.5 M NaCl solution at  $-0.9 \text{ V}$  (SCE) as a function of the electrode surface roughness ( $R_a$ ).

the measured electrode capacitance (Fig. 6). On the other hand, the anodic polarization curves obtained with electrodes kept for different lengths of time in distilled water (Fig. 10) practically overlap indicating that the dissolution rate is controlled only by processes in the compact, barrier layer.

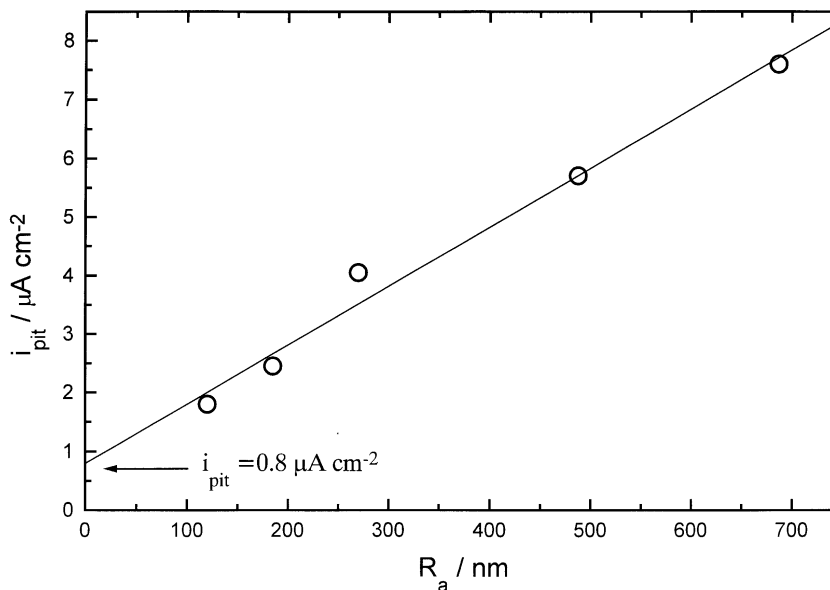


Fig. 9. The same as in Fig. 8 but at  $E_{\text{pit}} = -0.76 \text{ V}$  (SCE).

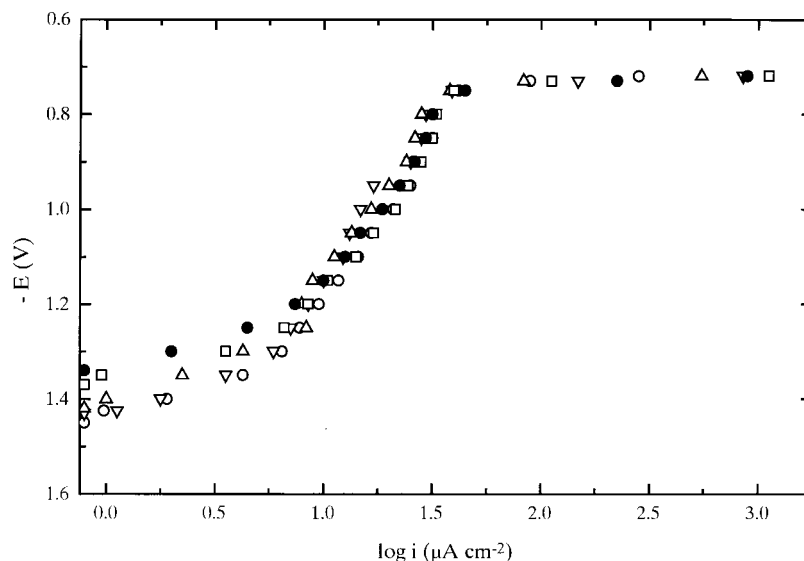


Fig. 10. Anodic polarization curves for Al in deaerated 0.5 M NaCl solution. Before the measurement the electrodes had been in contact with water for: (o) – 1 h; (□) – 24 h; (▽) – 82 h; (Δ) – 120 h and (●) – 192 h.

#### DISCUSSION

It can be concluded that prolonged action of the environment, (see Fig. 5) results only in an increase of the thickness of the porous part of the film (in the form of amorphous hydroxide  $\text{Al}(\text{OH})_3$  or crystalline bayerite  $\text{Al}_2\text{O}_3 \cdot 3\text{H}_2\text{O}$ ) while the thickness of the barrier layer seems to remain more or less constant, judging from the very similar and constant values of the electrode capacitances. Also, Fig. 10 shows that differences in the thickness of the porous part of the film does not affect the anodic polarization of Al. On the other hand, as we have shown elsewhere,<sup>6</sup> changes in the barrier layer thickness affect the anodic dissolution rate. This was interpreted by a model in which the anodic dissolution is controlled by the ionic charge transfer through the metal/oxide or oxide/solution interfaces.<sup>5,6</sup> Since prolonged contact with distilled water and air did not change the electrode capacitance (see Fig. 5) and anodic behavior (see Fig. 10), it is reasonable to assume that the effective electrode capacitance is determined by the thickness and relative permittivity of the barrier layer.

The thickness of this layer at the corrosion potential can be calculated from the estimated capacitance of the ideally flat surface  $C_T = 3.76 \mu\text{F cm}^{-2}$ . This total electrode capacitance can be considered to be the result of two, in series connected capacitances, the one corresponding to the barrier layer,  $C_{\text{ox}}$ , and the second one to the double layer capacitance of the oxide/electrolyte interface,  $C_{\text{dl}}$ ; *i.e.*,  $1/C_T = 1/C_{\text{ox}} + 1/C_{\text{dl}}$ . Taking that  $C_{\text{dl}} = 20 \mu\text{F cm}^{-2}$ , one calculates for the barrier layer capacitance  $C_{\text{ox}} = 4.63 \mu\text{F cm}^{-2}$ . The barrier layer is a good example of a parallel plate condenser,



*i. e.*,  $C_{\text{ox}} = \epsilon_0 \epsilon_r / d_{\text{ox}}$ . In the literature<sup>9</sup> value of the relative permittivity of the  $\text{Al}_2\text{O}_3$  oxide is quoted as lying between 8 and 10.6. Taking the permittivity of vacuum as  $\epsilon_0 = 8.85 \times 10^{-12} \text{ A s V}^{-1} \text{ m}^{-1}$ , and  $\epsilon_r = 10$ , the barrier layer thickness as  $d_{\text{ox}} = 1.89 \text{ nm}$  can be calculated. Bearing in mind the possible errors in the estimate of the used values for  $C_{\text{ox}}$  and  $\epsilon_r$  it can be concluded that the real thickness of the barrier layer, which controls the anodic dissolution process, is *ca.* 2 nm.

*Acknowledgement:* This work was financially supported by the Ministry of Science and Technology of Serbia.

## ИЗВОД

СТВАРНА ПОВРШИНА ЕЛЕКТРОДЕ ОД АЛУМИНИЈУМА У РАСТВОРУ  
НАТРИЈУМ-ХЛОРИДА

Д. М. ДРАЖИЋ,<sup>1</sup> Ј. П. ПОПИЋ<sup>1</sup> и З. РАКОЧЕВИЋ<sup>2</sup>

<sup>1</sup>ИХТМ-Центар за електрохемију, Њеђошева 12, б.бр. 815, 11001 Београд и  
<sup>2</sup>Институт за нуклеарне науке "Винча", б.бр. 522, 11001 Београд

Показано је, комбинованим коришћењем техника споре потенциодинамике, АС импеданце и атомске микроскопије (AFM), да су разлике у брзинама анодног растварања Al у 0,5 М NaCl у области између корозионог и питинг потенцијала, а које се запајају у експериментима, првенствено последица разлике у површинској храпавости различито припремљених електрода. Показано је да се механичким брушењем (финоћа 400) и полирањем  $\text{Al}_2\text{O}_3$  пастом (0,25  $\mu\text{m}$ ) добија разлика фактора храпавости за око 6 пута. Уз помоћ AFM технике за одређивање фактора храпавости процењена је права капацитивност електрода од 4,63  $\mu\text{F cm}^{-2}$  и дебљина баријерног слоја оксида од  $d_{\text{ox}} \approx 2,0 \text{ nm}$ . Спољашњи порозни слој је делимично аморфан  $\text{Al}(\text{OH})_3$  или кристалични бајерит ( $\text{Al}_2\text{O}_3 \cdot 3\text{H}_2\text{O}$ ).

(Примљено 10. јула 1999)

## REFERENCES

1. J. Kunze, *Corros. Sci.* **7** (1967) 273
2. S. E. Frers, M. M. Stefanel, C. Mayer, T. Chierchie, *J. Appl. Electrochem.* **20** (1990) 996
3. C. M. A. Brett, *J. Appl. Electrochem.* **20** (1990) 1000
4. A. R. Despić, J. Radošević, M. Kliškić, 7<sup>th</sup> *European Symposium of Corrosion Inhibitors (7SEIC)*, Ann. Univ. Ferrara, N. S. Sez. V. Suppl. N. 9, (1990) 1119
5. D. M. Dražić, J. P. Popić *J. Serb. Chem. Soc.* **59** (1994) 755
6. D. M. Dražić, J. P. Popić, *J. Serb. Chem. Soc.* **58** (1993) 791
7. A. Guntershultze, H. Betz, *Z. Physik* **91** (1932) 367
8. R. K. Hart, *Trans. Faraday Soc.* **53** (1957) 1020
9. R. S. Alwitt, *J. Electrochem. Soc.* **118** (1971) 1730
10. R. S. Alwitt, *The Aluminium-Water System in Oxides and Oxide Film*, Vol. 4, J. W. Diggle, A. S. Wijn, Eds., Marcel Dekker, New York, 1976, p. 169
11. J. P. Popić, *Ph. D. Thesis*, University of Belgrade, Belgrade, 1998
12. R. M. Stevanović, A. R. Despić, D. M. Dražić, *Electrochim. Acta* **33** (1988) 397
13. S. Trasatti, O. A. Petrii, *Pure&Appl.Chem.* **63** (1991) 711.